ChemComm

COMMUNICATION

View Article Online
View Journal | View Issue

Photoenolization *via* excited state double proton transfer induces "turn on" fluorescence in diformyl diaryl dipyrromethane†

Cite this: *Chem. Commun.*, 2014, 50, 8667

Received 14th May 2014, Accepted 13th June 2014

DOI: 10.1039/c4cc03668a

www.rsc.org/chemcomm

K. C. Gowri Sreedevi,[a] Ajesh P. Thomas,[b] K. H. Aparna,[b] Renuka Pradhan,[b] M. L. P. Reddy,[a] U. Lourderaj[b] and A. Srinivasan*[b]

A light triggered enolization in diformyl diaryl dipyrromethane by excited state dual proton transfer (ESDPT) induces "turn on" fluorescence. The role of diaryl and diformyl groups in the enolization process was confirmed by photophysical and theoretical studies.

Certain molecular systems change their chemical structures in response to external stimuli such as chemical, electrical or light thereby modulating their luminescence properties.[1] In particular, light stimulated responses resulting in irreversible[2a] or reversible[2b] structural and conformational changes play a major role in the precise analysis of biological functions.[2] One such structural transformation is the photoinduced proton transfer, involved in several biochemical reactions in living systems.[3]

Recently, a computational study on pyrrole-2-carboxaldehyde (P2C), a nonfluorescent molecule commonly used in the synthesis of porphyrins,[4] predicted the possibility of an excited state intra- or inter-molecular proton transfer from NH to CO forming enol.[5] However, such a proton transfer process has not been observed experimentally in pyrrole derivatives to date. Herein, we report a case of light activated fluorescent "turn on" caused by the photoinduced excited state intramolecular dual proton transfer (ESDPT) in 1,9-diformyl-5,5-diaryldipyrromethane (**DA$_{KK}$**) resulting in a dienol that exhibits a large Stokes shifted emission. Interestingly, it is found that the photoenolization is favored by the presence of aryl substituents at the *meso*-carbon.

Vilsmeier–Haack formylation of ditolyldipyrromethane[6] using DMF and $POCl_3$ at 0 °C for 1 h resulted in **DA$_{KK}$** (72% yield) and was characterized by ^1H NMR, ^{13}C NMR, FAB mass spectrometry (Fig. S1–S3, ESI†) and finally confirmed by single-crystal X-ray-diffraction analysis (Fig. 1a).

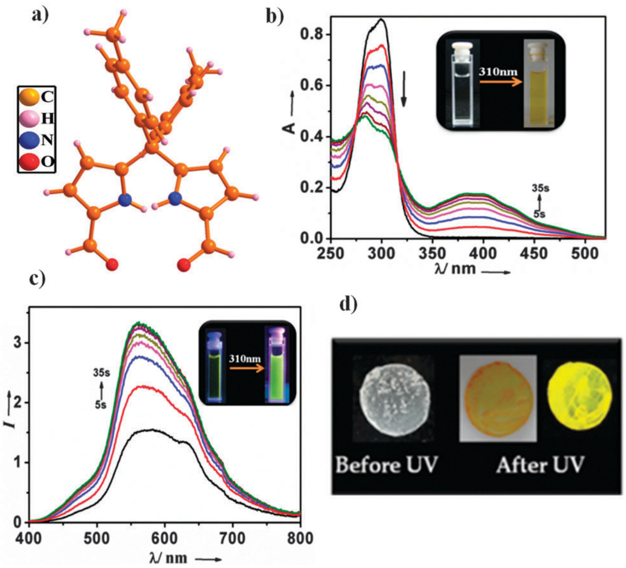

Fig. 1 (a) Single crystal X-ray structure of **DA$_{KK}$**, (b) absorption and (c) emission changes of **DA$_{KK}$** (2.75×10^{-5} M) in acetonitrile upon UV irradiation along with visible color and emission changes (inset). (d) The solid state color change of **DA$_{KK}$** before and after UV irradiation under visible and UV light.

The UV-Vis absorption spectrum of **DA$_{KK}$** in acetonitrile showed an absorption maximum at 300 nm ($\varepsilon = 3.3 \times 10^4\ M^{-1}\ cm^{-1}$) which was assigned to a π–π^* transition and a very weak emission band at around 560 nm, when excited at the absorption maximum. However, the fluorescence excitation spectrum (λ_{em} = 560 nm) showed a band between 380–500 nm with two peaks (Fig. S4, ESI†) that differed largely from the absorption spectrum of **DA$_{KK}$**, predicting the presence of a new species. Further, when a 2.75×10^{-5} M solution of **DA$_{KK}$** in acetonitrile was exposed to UV irradiation for definite time intervals with a band-pass filter $\lambda = 300 \pm 20$ nm, the absorption band at 300 nm decreased gradually with the appearance of a new broad band with maximum intensity at 390 nm. UV irradiation was accompanied by a color change from colorless to bright yellow (Fig. 1b, inset) and exhibited a clear isosbestic point at 316 nm.

---

[a] *School of Chemical Sciences, National Institute of Science Education and Research (NISER), Bhubaneswar-751005, Orissa, India. E-mail: srini@niser.ac.in*

[b] *Chemical Science and Technology Division, National Institute for Interdisciplinary Science and Technology (NIIST-CSIR), Trivandrum-695019, Kerala, India*

† Electronic supplementary information (ESI) available: Spectral details, coordinates of minimum energy structures, and details of photoirradiation studies of **DA$_{KK}$**. CCDC 923773. For ESI and crystallographic data in CIF or other electronic format see DOI: 10.1039/c4cc03668a

The appearance of a new red-shifted absorption peak (390 nm) in the excitation spectrum supports the formation of a new species. The fluorescence intensity at 560 nm enhanced continuously with bright green emission (Fig. 1c, inset) and a fourfold increase in the fluorescence quantum yield ($\phi_f = 0.02$) with respect to fluorescein. Moreover, the new species formed was found to be solid state emissive (Fig. 1d), which can potentially be applicable in the fabrication of luminophore based devices, where the solid state emission is desirable.[7] It should be pointed that **DA$_{KK}$** with other external stimuli such as heat and pH variation did not show any change in the absorption/emission spectra. The reversibility of the processes was also checked with visible light irradiation, heat/dark and was found to be irreversible.

Two possible mechanisms were considered to explain the observed photophysical changes upon irradiation: (i) keto–enol tautomerization by proton transfer from the pyrrolic NH to carbonyl CO group to generate enol and (ii) *cis–trans* isomerization of the CO group with respect to NH,[8] where *cis* refers to the CO group *syn* to NH, and *trans* refers to the CO group *anti* to NH. The ^{1}H NMR spectrum of **DA$_{KK}$** in CD_3CN before and after irradiation (Fig. S5a and b, ESI†) showed a distinct difference. Before irradiation, the formyl proton appeared at 9.41 ppm and the NH proton at 9.72 ppm. ^{1}H NMR spectra after irradiation displayed several additional peaks indicating a mixture of compounds, possibly the diketo and a newly formed species. The IR spectrum of **DA$_{KK}$** before irradiation showed the CO stretching frequency at 1656 cm^{-1} and a broad peak for NH at 3211 cm^{-1} along with a shallow peak at 3435 cm^{-1} (Fig. S6, ESI†). However, the IR spectrum after irradiation showed a weak NH band (3227 cm^{-1}) and an intense broad band at 3436 cm^{-1} that can be assigned to the O–H stretching band, indicating the formation of enolic species. To confirm that irradiation results in the formation of enol, it is important to ascertain the role of the NH proton in the process. This was investigated by the addition of a strong base such as F$^-$ ions (as its tetrabutylammonium salt) to an acetonitrile solution of **DA$_{KK}$** prior to UV irradiation. The abstraction of NH by the base was confirmed by the disappearance of the NH proton peak in the ^{1}H NMR spectrum (Fig. S7, ESI†). Interestingly, UV irradiation after the deprotonation did not result in the "turn on" emission, indicating the role of NH proton in the formation of the new species. The fact that the abstraction of protons by a base can inhibit the keto–enol tautomerism and the absence of "turn on" emission rule out the possibility of *cis–trans* isomerization as the C–C single bond rotation does not depend on the presence of the NH proton.

Solvent dependent analyses showed that the absorption and emission spectra of **DA$_{KK}$** after photoirradiation exhibited a positive solvatochromism (Fig. S8 and Table S1, ESI†). The large red shift in the λ_{em}^{max} suggested the excited state to be highly polar in nature than the ground state, confirming the involvement of a polar enolic species in the process further eliminating the possibility of *cis–trans* isomerization. Photophysical changes in **DA$_{KK}$** due to irradiation in a series of solvents of varying polarity (cyclohexane to DMSO) were monitored by the changes in the absorption maximum of the enol peak as a function of irradiation time (Fig. 2). The keto–enol tautomerism was found to follow the first-order kinetics[9] and the rate constant (k) values at 298 K increased with solvent polarity (Table S2, ESI†). The percentage of conversion from the diketo species in each solvent at the photostationary state was calculated from the decrease in optical density at 300 nm, which showed higher conversion in polar solvents.

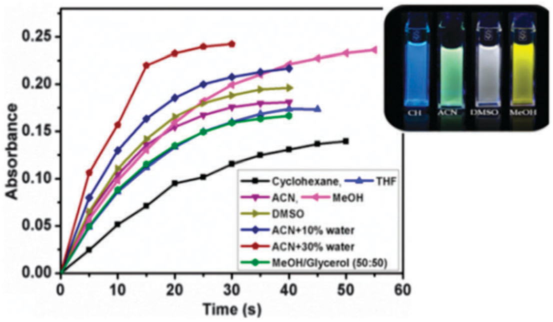

Fig. 2 Changes in the absorption maxima of **DA$_{KK}$** as a function of UV irradiation time. Inset: emission color change of **DA$_{KK}$** after irradiation in different solvents.

In order to analyse the role of the formyl group in the photo-induced keto–enol tautomerism, further investigation was done with other dipyrromethane derivatives such as **MF$_K$**, which have only one formyl group and **DT**, without any formyl groups (Scheme 1). The UV-Vis absorption spectra recorded for **MF$_K$** (2.75×10^{-5} M) in acetonitrile exhibited a peak at 297 nm which decreased gradually with a concomitant increase at 370 nm upon UV irradiation with an isosbestic point at 317 nm (Fig. S9, ESI†). However, the photostationary state was achieved only after 11 min compared to 35 s in **DA$_{KK}$** and the irradiated solution of **MF$_K$** remained colorless with a weak emission at 439 nm. In contrast, **DT** showed no significant change in the absorption spectra upon irradiation, further confirming the importance of diformyl substitution and thus the formation of enolic species by a proton transfer process. Also, the significance of aryl substitution at the *meso*-carbon in the photoenolization was studied with **MA$_{KK}$**, which has only one aryl group at the *meso*-carbon and **DM$_{KK}$**, where aryl groups are replaced with methyl groups (Scheme 1). There was no appreciable change observed in the absorption spectrum for **MA$_{KK}$** even after 10 min of irradiation (Fig. S10, ESI†). In the case of **DM$_{KK}$**, a continuous decrease in absorbance was observed without any color change.

Density functional theoretical (DFT) calculations were performed to gain a better insight into the keto–enol tautomerization process, particularly to understand the role of diaryl substitution at the *meso*-carbon of **DA$_{KK}$** in the enolization process by using the B3LYP functional and 6-31+G* basis set.[10] Although the absorption and

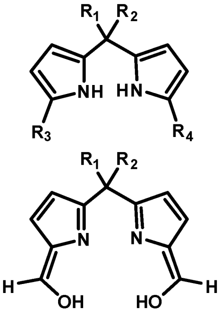

DA$_{KK}$: $R_1 = R_2 = (p\text{-}CH_3)C_6H_4$, $R_3 = R_4 =$ CHO
DM$_{KK}$: $R_1 = R_2 = CH_3$, $R_3 = R_4 =$ CHO
DH$_{KK}$: $R_1 = R_2 =$ H, $R_3 = R_4 =$ CHO
MF$_K$: $R_1 = R_2 = (p\text{-}CH_3)C_6H_4$, $R_3 =$ CHO, $R_4 =$ H
MA$_{KK}$: $R_1 = C_6H_5$, $R_2 =$ H, $R_3 = R_4 =$ CHO
DT: $R_1 = R_2 = (p\text{-}CH_3)C_6H_4$, $R_3 = R_4 =$ H

DA$_{EE}$: $R_1 = R_2 = (p\text{-}CH_3)C_6H_4$
DM$_{EE}$: $R_1 = R_2 = CH_3$
DH$_{EE}$: $R_1 = R_2 =$ H

Scheme 1 Keto and enol forms of dipyrromethanes considered in this study.

Table 1 Relative energy, absorption and emission properties of KK and EE tautomers of **DH**, **DM** and **DA** computed at the B3LYP/6-31+g* level of theory

Molecule	DH		DM		DA	
Tautomer	KK	EE	KK	EE	KK	EE
Relative energy (kcal mol^{-1})						
S_0	0.0	34.0	0.0	34.0	0.0	35.9
S_1	0.0	28.5	0.0	27.6	0.0	20.0
Vertical excitation wavelength (nm)						
S_1	316	318	316	319	318	345
S_2	316	309	316	310	318	330
S_3	293	306	295	306	302	327
$\lambda_{abs}{}^{a}$	—	—	$<$250	—	300	390
Emission wavelength (nm)						
λ_{em}	386	507	385	521	386	327
$\lambda_{em}{}^{b}$	—	—	—	—	—	560

[a] Experimental absorption maximum. [b] Experimental emission maximum.

emission wavelengths may not match with the experiments owing to the gas-phase nature of the calculations, qualitative and important insight into the experimental observations can be deduced from the DFT results. The ground and excited state minimum energy structures of $\mathbf{DA_{EE}}$ showed distinct differences in the orientation of the aryl and pyrrole rings (Fig. S12, ESI†). The relative energy calculations showed that in the ground state, the $\mathbf{DA_{EE}}$, $\mathbf{DM_{EE}}$ and $\mathbf{DH_{EE}}$ are $\sim$34.0 kcal mol^{-1} higher in energy than the KK forms irrespective of the *meso*-carbon substitution (Table 1).

The computed excitation energies and the molecular orbitals contributing to the excitations are given in Table 1 and Fig. S13 (ESI†) respectively. It can be seen that for $\mathbf{DA_{KK}}$, the transitions resulted from charge redistribution in the pyrrole rings, whereas in $\mathbf{DA_{EE}}$, there is an extension of conjugation from pyrrole to the phenyl ring. For all the three KK structures, the S_1 and S_2 states are due to n–π* (HOMO − 6 to LUMO, HOMO − 6 to LUMO + 1, respectievely) transitions and are degenerate, while S_3 is due to π–π* (HOMO to LUMO) transition. In the case of EE structures, all the first three excited states are π–π* [HOMO to LUMO (S_1), HOMO − 1 to LUMO (S_2), and HOMO − 1 to LUMO + 1 (S_3)] in nature and the S_2 and S_3 states are nearly degenerate. The vertical excitation energies are similar (316–293 nm) for $\mathbf{DH_{KK}}$, $\mathbf{DM_{KK}}$, and $\mathbf{DA_{KK}}$, again showing the absence of substituent effects in the excited states of the KK forms (Table 1). The enols, $\mathbf{DH_{EE}}$ and $\mathbf{DM_{EE}}$ also showed similar absorption energies (319–306 nm) and interestingly these are also similar to those of the KK forms. However, $\mathbf{DA_{EE}}$ showed a red shift of 43 nm (λ = 345 nm) compared to that of the π–π* (S_3) state of $\mathbf{DA_{KK}}$.

The red shift in the vertical absorption wavelength seen in $\mathbf{DA_{EE}}$ is consistent with the experimental observation and can be attributed to the extended charge delocalization seen in the π-orbitals of the pyrrole and the aryl rings that are involved in the transitions in $\mathbf{DA_{EE}}$. The emission energies of the KK forms of all the three molecules are similar ($\sim$386 nm) indicating that there is little effect of the substituents on their emission properties. The emission wavelengths calculated for $\mathbf{DH_{EE}}$, $\mathbf{DM_{EE}}$ and $\mathbf{DA_{EE}}$ are 507, 521 and 527 nm, respectively, and can be compared to the experimental emission maximum of 560 nm for $\mathbf{DA_{EE}}$ (Table 1). Clearly, the DFT calculations reiterate that the appearance of the new red shifted peak is due to the formation of the enolic tautomer.

The relative energies (Table 1) of the EE minima in the S_1 state revealed that $\mathbf{DH_{EE}}$ and $\mathbf{DM_{EE}}$ are $\sim$29 kcal mol^{-1} higher than that of the KK form, whereas only $\sim$20 kcal mol^{-1} for $\mathbf{DA_{EE}}$. The additional stabilization of $\sim$10 kcal mol^{-1} seen in $\mathbf{DA_{EE}}$ clearly demonstrates that the KK to EE tautomerization of **DA** in the S_1 state is energetically more favorable compared to that of **DH** and **DM** systems. Although the tautomerization barrier in the S_1 state could not be calculated, it can be expected that such stabilization of the transition state connecting the KK and EE forms may be seen for **DA**. The above results explain the appearance of a new red shifted absorption due to enol formation and the importance of aryl substitution to enable keto–enol tautomerization in the excited state, a phenomenon not seen for other derivatives. The complete photophysical processes during irradiation of **DH** and **DA** systems are given in Fig. S14 (ESI†) for comparison.

To summarize, we have demonstrated the photoenolization of **DA**, *via* ESDPT. To the best of our knowledge, this is the first report on light triggered enolization of a dipyrromethane derivative with ''turn on'' fluorescence and emissive even in the solid state. DFT calculations confirm the importance of the diaryl group at the *meso*-carbon that stabilizes the dienol form in the excited state compared to monoaryl or dimethyl groups. In future, the application of the light triggered large Stokes-shifted emission of the molecule as sensors will be explored.

KCGS, APT and RP thank CSIR, New Delhi, for fellowship. We thank Dr Arun Kumar, NISER, for X-ray structure of **DA**.

Notes and references

1 (*a*) Y. Sagara and T. Kato, *Nat. Chem.*, 2009, **1**, 605; (*b*) H. Maeda, Y. Bando, K. Shimomura, I. Yamada, M. Naito, K. Nobusawa, H. Tsumatori and T. Kawai, *J. Am. Chem. Soc.*, 2011, **133**, 9266.

2 (*a*) G. Mayer and A. Heckel, *Angew. Chem., Int. Ed.*, 2006, **45**, 4900; (*b*) Q. Chen, D. Zhang, G. Zhang, X. Yang, Y. Feng, Q. Fan and D. Zhu, *Adv. Funct. Mater.*, 2010, **20**, 3244; (*c*) T. Kobayashi, T. Komatsu, M. Kamiya, C. Campos, M. González-Gaitán, T. Terai, K. Hanaoka, T. Nagano and Y. Urano, *J. Am. Chem. Soc.*, 2012, **134**, 11153.

3 (*a*) D. R. Morris and L. P. Hager, *J. Biol. Chem.*, 1966, **241**, 3582; (*b*) A. Taurog, *Endocrinology*, 1976, **98**, 1031; (*c*) S. A. Aziz and C. O. Knowles, *Nature*, 1973, **242**, 417–418.

4 (*a*) H. Fischer and W. Gleim, *Justus Liebigs Ann. Chem.*, 1935, **521**, 157; (*b*) A. Wiehe, C. Ryppa and M. O. Senge, *Org. Lett.*, 2002, **4**, 3807.

5 N. Kumar, S. Chakravorti and P. Chowdhury, *J. Mol. Struct.*, 2008, **891**, 351.

6 K. C. G. Sreedevi, A. P. Thomas, P. S. Salini, S. Ramakrishnan, K. S. Anju, M. G. D. Holaday, M. L. P. Reddy, C. H. Suresh and A. Srinivasan, *Tetrahedron Lett.*, 2011, **52**, 5995.

7 R. Deans, J. Kim, M. R. Machacek and T. M. Swager, *J. Am. Chem. Soc.*, 2000, **122**, 8565.

8 (*a*) C. A. Rice, I. Dauster and M. A. Suhm, *J. Chem. Phys.*, 2007, **126**, 134313; (*b*) B. M. Giuliano, I. Reva and R. Fausto, *J. Phys. Chem. A*, 2010, **114**, 2506.

9 Y. Chiang, A. J. Kresge, Q. Meng, R. A. More O'Ferrall and Y. Zhu, *J. Am. Chem. Soc.*, 2001, **123**, 11562.

10 (*a*) A. D. Becke, *J. Chem. Phys.*, 1993, **98**, 5648; (*b*) P. J. Stephens, F. J. Devlin, C. F. Chablowski and M. J. Frisch, *J. Phys. Chem.*, 1994, **98**, 11623; (*c*) R. H. Hertwig and W. Koch, *Chem. Phys. Lett.*, 1997, **268**, 345.